Supplementary Information

Symmetry and Substituent Electronics Dictate Electronic Structure of Low Spin, Mixed-ring Rhenocene Complexes

Eyram Asempa[1,†], Gregory M. Curtin[1,2,†], Ann Marie May[2,†], Jillian L. Dempsey[2], and Elena Jakubikova*[1]*

[1] Department of Chemistry, North Carolina State University, Raleigh, North Carolina 27695, United States

[2] Department of Chemistry, University of North Carolina at Chapel Hill, Chapel Hill, North Carolina 27599-3290, United States

Table of Contents

Table S1. Re–C bond lengths for the DFT-optimized structures of Re(Cp)(CpMe$_4$R) complexes, where R = Me (1), CF$_3$ (2), ^{t}Bu(3), CHCH$_2$ (4), CHO (5) and OMe (6). See Figure S3 for C atom labels. Re–L distances correspond to the distance between the Re atom and the centroid (Cen) of the Cp or CpMe$_4$R ring defined by the five carbon atoms in the ring. S3

Figure S1. Fragmentation scheme utilized to determine the localization of MOs in complexes 1-6 (orange: Cp, green: CpMe$_4$R, blue: Re). The figure also shows atom and ring centroid labels utilized in Table S1..... S3

Figure S2. Energy level diagram of the doublet ground states of 4, 5 and 6 using B3LYP+D2/6-311G*, SDD(Re) in benzene. MOs with > 70% localization on the metal center are labeled in blue, those with > 50% localization on Cp are shown in orange, and MOs with > 45% localization on CpMe$_4$R are shown in green. S4

Figure S3. Energy level diagram of the doublet ground state of the complexes 1-6. ..... S4

Figure S4. α molecular orbitals of Re(Cp)(CpMe$_4$R) complexes where R = Me (1), CF$_3$ (2), ^{t}Bu(3), CHCH$_2$ (4), CHO (5) and OMe (6) S5

Figure S5. β molecular orbitals of Re(Cp)(CpMe$_4$R) complexes where R = Me (1), CF$_3$ (2), ^{t}Bu(3), CHCH$_2$ (4), CHO (5) and OMe (6) S6

Figure S6. βHOMO-LUMO gap of Re(Cp)(CpMe$_4$R) complexes where R = Me (1), CF$_3$ (2), ^{t}Bu(3), CHCH$_2$ (4), CHO (5) and OMe (6) S6

Table S2. α-fragment molecular orbital analysis of Re(Cp)(CpMe$_4$R), where R = Me (1) S7

Table S3. α-fragment molecular orbital analysis of Re(Cp)(CpMe$_4$R), where R = CF$_3$ (2)..... S7

Table S4. α-fragment molecular orbital analysis of Re(Cp)(CpMe$_4$R), where R = ^{t}Bu (3)..... S7

Table S5. α-fragment molecular orbital analysis of Re(Cp)(CpMe$_4$R), where R = CHCH$_2$ (4)..... S7

Table S6. α-fragment molecular orbital analysis of Re(Cp)(CpMe$_4$R), where R = CHO (5)..... S8

Table S7. α-fragment molecular orbital analysis of Re(Cp)(CpMe$_4$R), where R = OMe (6)..... S8

Table S8. β-fragment molecular orbital analysis of Re(Cp)(CpMe$_4$R), where R = Me (1)..... S8

Table S9. β-fragment molecular orbital analysis of Re(Cp)(CpMe$_4$R), where R = CF$_3$ (2)..... S8

Table S10. β-fragment molecular orbital analysis of Re(Cp)(CpMe$_4$R), where R = ^{t}Bu(3)..... S9

Table S11 β-fragment molecular orbital analysis of Re(Cp)(CpMe$_4$R), where R = CHCH$_2$ (4).... S9

Table S12. β-fragment molecular orbital analysis of Re(Cp)(CpMe$_4$R), where R = CHO (5)..... S9

Table S13. β-fragment molecular orbital analysis of Re(Cp)(CpMe$_4$R), where R = OMe (6)..... S9

Figure S7. Donor and acceptor orbitals of the lowest energy excited states for complexes 4-6. Calculated excitation energies (in nm) and oscillator strengths (f) for each electronic transition are provided. The percent contribution of the displayed hole-particle pair determined from the excitation coefficients obtained from the TD-DFT calculations is also provided..... S10

Table S14. Excited states for 1. Excited states were characterized for wavelengths > 400 nm with oscillator strength (f) ≥ 0.00..... S11

Table S15. Excited states for 2. Excited states were characterized for wavelengths > 400 nm with oscillator strength (f) ≥ 0.00 ..... S12

Table S16. Excited states for 3. Excited states were characterized for wavelengths > 400 nm with oscillator strength (f) ≥ 0.00 ..... S13

Table S17. Excited states for 4. Excited states were characterized for wavelengths > 400 nm with oscillator strength (f) ≥ 0.00..... S14

Table S18. Excited states for 5. Excited states were characterized for wavelengths > 400 nm with oscillator strength (f) ≥ 0.00..... S15

Table S19. Excited states for 6. Excited states were characterized for wavelengths > 400 nm with oscillator strength (f) ≥ 0.00..... S17

Table S20. Table of Calculated DFT Energies S18

Table S1. Re–C bond lengths for the DFT-optimized structures of Re(Cp)($CpMe_4R$) complexes, where R = Me (**1**), CF_3 (**2**), ^tBu(**3**), $CHCH_2$ (**4**), CHO (**5**) and OMe (**6**). See Figure S3 for C atom labels. Re–L distances correspond to the distance between the Re atom and the centroid (Cen) of the Cp or $CpMe_4R$ ring defined by the five carbon atoms in the ring.

	Complex	1	2	3	4	5	6
Re-Cp bond lengths [Å]	**Re-C_1**	2.25	2.24	2.23	2.24	2.24	2.23
	Re-C_2	2.25	2.28	2.27	2.25	2.29	2.28
	Re-C_3	2.25	2.34	2.34	2.32	2.34	2.35
	Re-C_4	2.25	2.34	2.35	2.35	2.32	2.35
	Re-C_5	2.25	2.28	2.28	2.30	2.27	2.28
Re-$CpMe_4R$ bond lengths [Å]	**Re-C_1'**	2.24	2.16	2.20	2.22	2.20	2.17
	Re-C_2'	2.24	2.24	2.25	2.22	2.25	2.24
	Re-C_3'	2.24	2.33	2.32	2.30	2.33	2.32
	Re-C_4'	2.24	2.33	2.32	2.33	2.32	2.32
	Re-C_5'	2.24	2.24	2.24	2.27	2.23	2.24
Re-L distances [Å]	**Re-X**	1.89	1.95	1.95	1.94	1.95	1.95
	Re-X'	1.87	1.90	1.90	1.91	1.91	1.90
Angles [deg]	**X-Re-X'**	179.8	179.6	180.0	179.6	177.5	179.2
	X'-C_1'-R	175.6	171.0	167.8	174.6	177.6	172.9

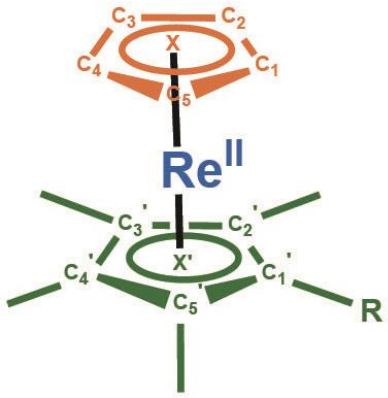

Figure S1. Fragmentation scheme utilized to determine the localization of MOs in complexes **1-6** (orange: Cp, green: $CpMe_4R$, blue: Re)**.** The figure also shows atom and ring centroid labels utilized in Table S1.

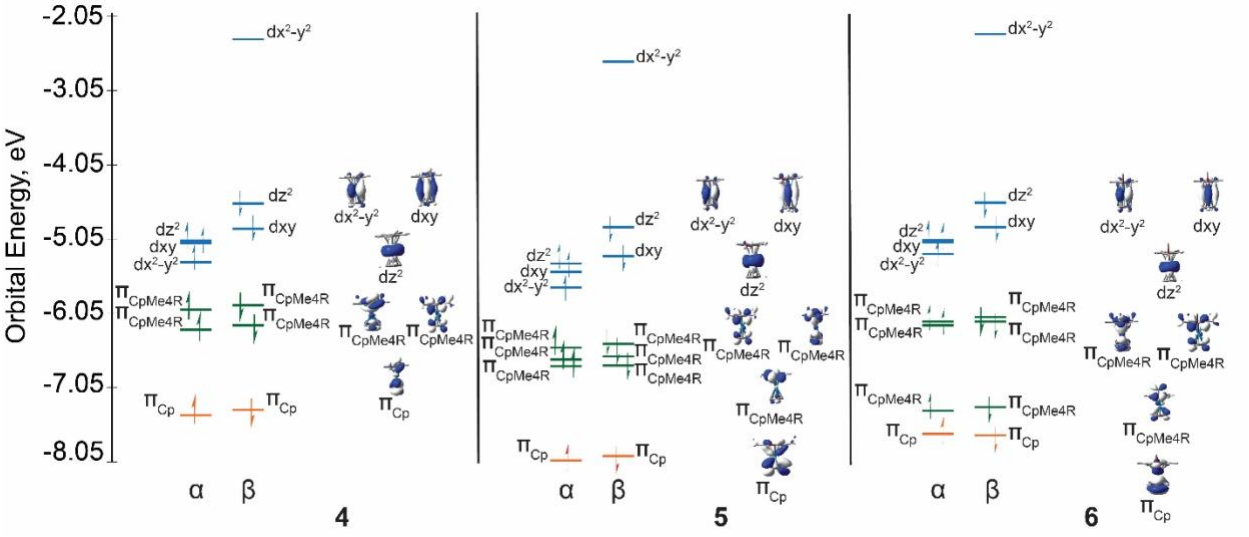

Figure S2. Energy level diagram of the doublet ground states of **4**, **5** and **6** using B3LYP+D2/6-311G*, SDD(Re) in benzene. MOs with > 70% localization on the metal center are labeled in blue, those with > 50% localization on Cp are shown in orange, and MOs with > 45% localization on $CpMe_4R$ are shown in green.

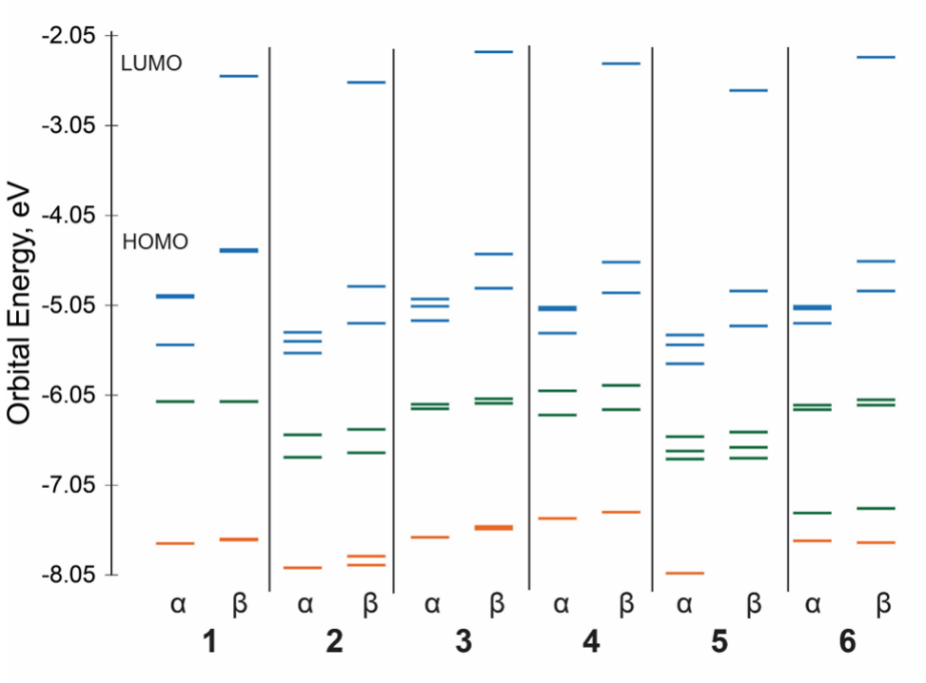

Figure S3. Energy level diagram of the doublet ground state of the complexes **1-6**.

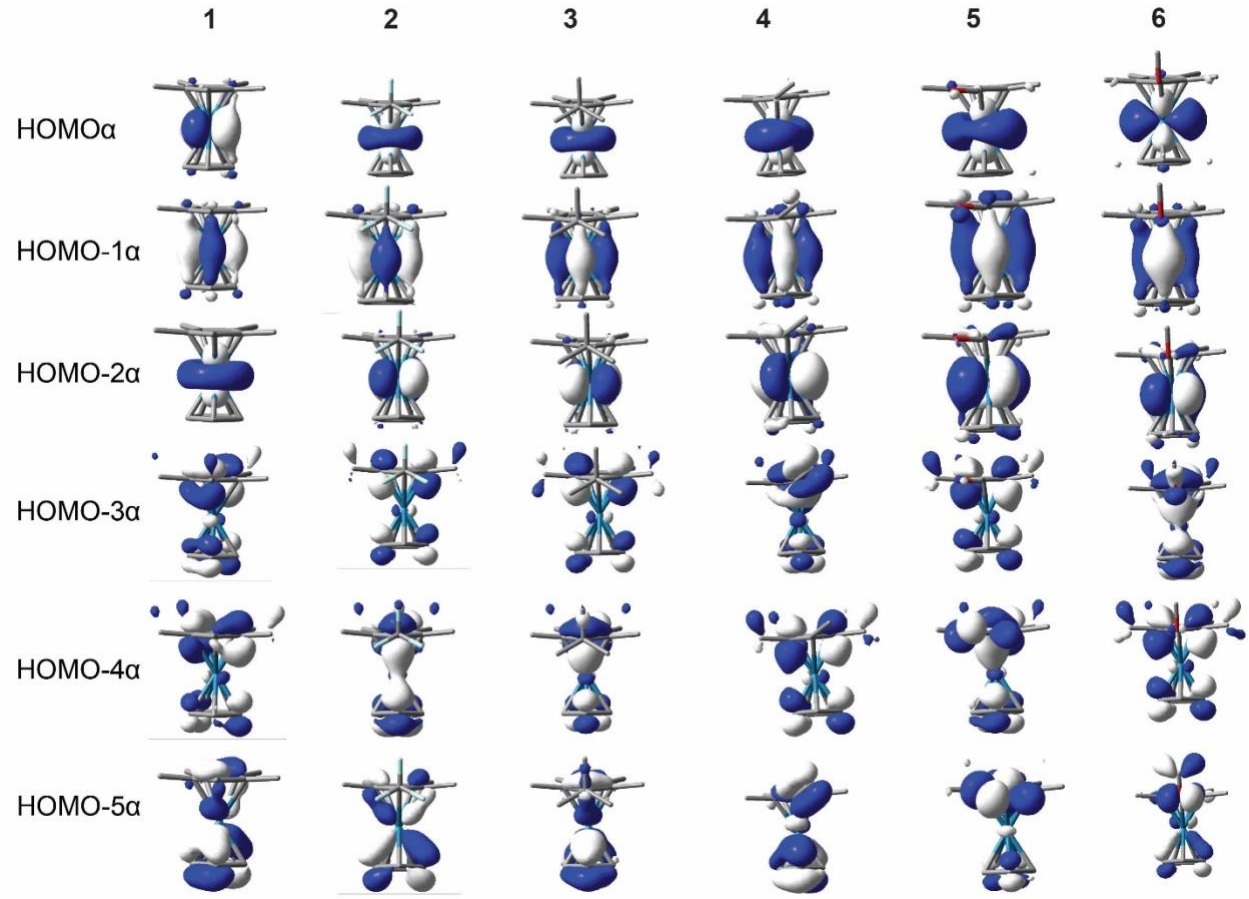

Figure S4. α molecular orbitals of Re(Cp)(CpMe$_4$R) complexes where R = Me (**1**), CF_3 (**2**), ^{t}Bu(**3**), $CHCH_2$ (**4**), CHO (**5**) and OMe (**6**)

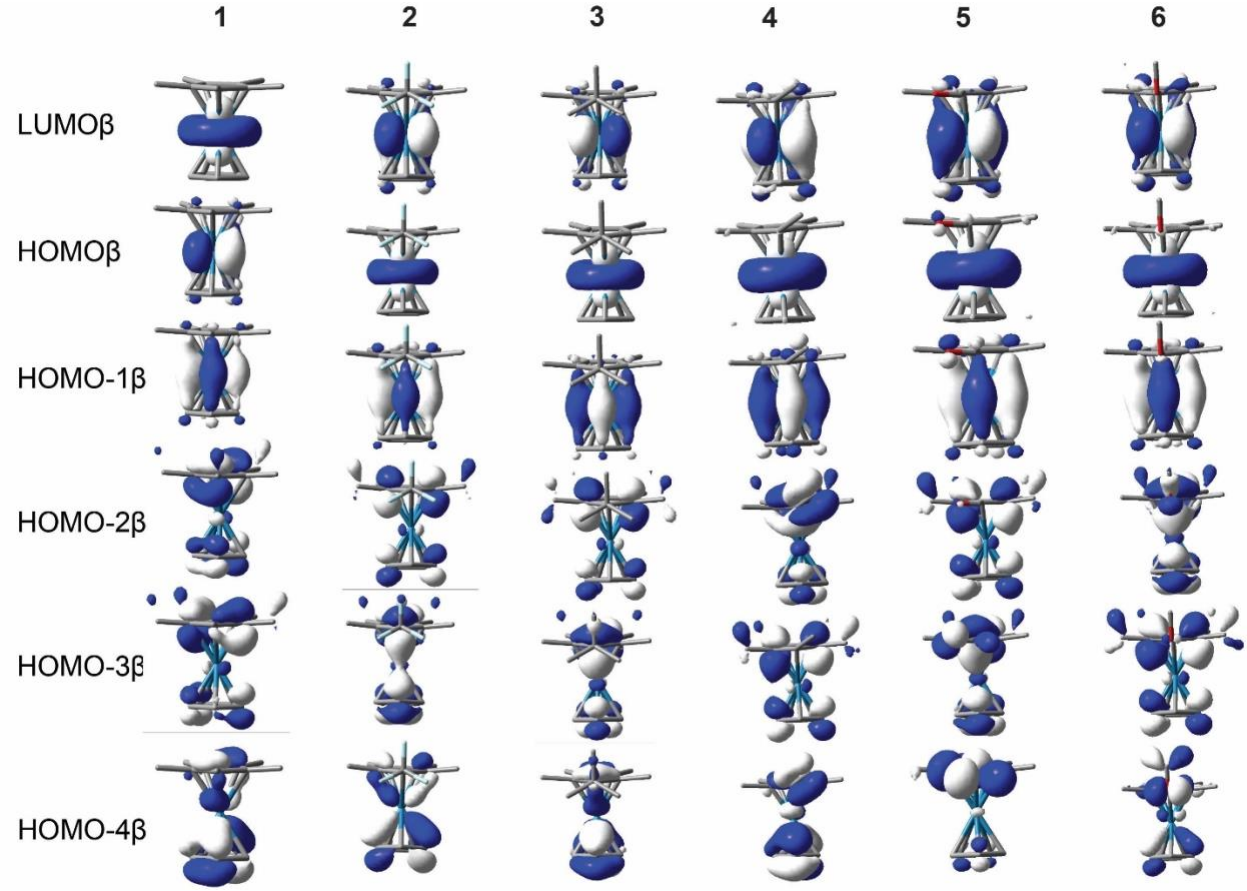

Figure S5. β molecular orbitals of Re(Cp)(CpMe$_4$R) complexes where R = Me (**1**), CF_3 (**2**), ^{t}Bu(**3**), $CHCH_2$ (**4**), CHO (**5**) and OMe (**6**)

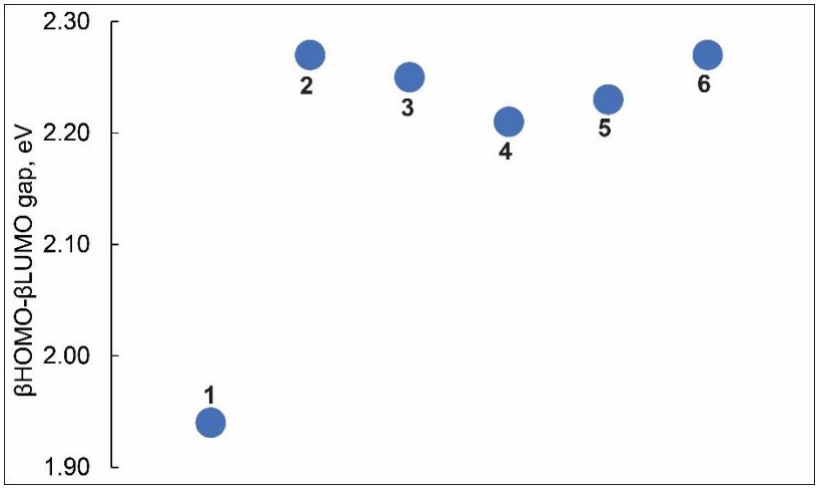

Figure S6. βHOMO-LUMO gap of Re(Cp)(CpMe$_4$R) complexes where R = Me (**1**), CF_3 (**2**), ^{t}Bu(**3**), $CHCH_2$ (**4**), CHO (**5**) and OMe (**6**)

Table S2. α-fragment molecular orbital analysis of Re(Cp)(CpMe$_4$R), where R = Me (**1**)

α MO	HOMO-5	HOMO-4	HOMO-3	HOMO-2	HOMO-1	HOMO
Energy (eV)	-7.70	-6.12	-6.12	-5.49	-4.95	-4.95
Re (%)	25	6	6	89	77	77
CpMe$_4$R (%)	23	61	61	7	12	12
Cp (%)	52	32	32	4	11	11

Table S3. α-fragment molecular orbital analysis of Re(Cp)(CpMe$_4$R), where R = CF_3 (**2**)

αMO	HOMO-5	HOMO-4	HOMO-3	HOMO-2	HOMO-1	HOMO
Energy (eV)	-7.97	-6.74	-6.49	-5.58	-5.45	-5.35
Re (%)	26	6	6	83	75	91
CpMe$_4$R (%)	24	53	60	9	15	6
Cp (%)	50	42	34	8	10	4

Table S4. α-fragment molecular orbital analysis of Re(Cp)(CpMe$_4$R), where R = ^{t}Bu (**3**)

α MO	HOMO-5	HOMO-4	HOMO-3	HOMO-2	HOMO-1	HOMO
Energy (eV)	-7.63	-6.20	-6.15	-5.22	-5.06	-4.98
Re (%)	23	6	6	82	77	91
CpMe$_4$R (%)	25	63	64	9	13	6
Cp (%)	52	31	30	8	11	3

Table S5. α-fragment molecular orbital analysis of Re(Cp)(CpMe$_4$R), where R = $CHCH_2$ (**4**)

α MO	HOMO-5	HOMO-4	HOMO-3	HOMO-2	HOMO-1	HOMO
Energy (eV)	-7.42	-6.27	-6.00	-5.36	-5.10	-5.07
Re (%)	12	6.09	7	83	76	90
CpMe$_4$R (%)	40	61	73	9	14	6
Cp (%)	48	33	21	8	10	4

Table S6. α-fragment molecular orbital analysis of Re(Cp)(CpMe$_4$R), where R = CHO (**5**)

α MO	HOMO-5	HOMO-4	HOMO-3	HOMO-2	HOMO-1	HOMO
Energy (eV)	-6.76	-6.67	-6.51	-5.70	-5.49	-5.58
Re (%)	3	3	6	83	75	89
CpMe$_4$R (%)	82	75	61	9	16	7
Cp (%)	15	22	33	8	9	4

Table S7. α-fragment molecular orbital analysis of Re(Cp)(CpMe$_4$R), where R = OMe (**6**)

α MO	HOMO-5	HOMO-4	HOMO-3	HOMO-2	HOMO-1	HOMO
Energy (eV)	-7.36	-6.21	-6.16	-5.25	-5.09	-5.09
Re (%)	5	6	6	82	79	89
CpMe$_4$R (%)	80	62	63	10	12	7
Cp (%)	15	32	31	8	9	5

Table S8. β-fragment molecular orbital analysis of Re(Cp)(CpMe$_4$R), where R = Me (**1**)

β MO	HOMO-4	HOMO-3	HOMO-2	HOMO-1	HOMO	LUMO
Energy (eV)	-7.65	-6.12	-6.12	-4.45	-4.44	-2.50
Re (%)	23	5	5	73	73	91
CpMe$_4$R (%)	23	63	63	14	14	6
Cp (%)	54	32	32	13	13	2

Table S9. β-fragment molecular orbital analysis of Re(Cp)(CpMe$_4$R), where R = CF$_3$ (**2**)

β MO	HOMO-4	HOMO-3	HOMO-2	HOMO-1	HOMO	LUMO
Energy (eV)	-7.65	-6.12	-6.12	-4.45	-4.44	-2.50
Re (%)	23	5	5	73	73	9
CpMe$_4$R (%)	23	63	63	14	14	6
Cp (%)	54	32	32	13	13	2

Table S10. β-fragment molecular orbital analysis of Re(Cp)(CpMe$_4$R), where R = ^{t}Bu(**3**)

β MO	HOMO-4	HOMO-3	HOMO-2	HOMO-1	HOMO	LUMO
Energy (eV)	-7.51	-6.14	-6.09	-4.86	-4.48	-2.23
Re (%)	22	5	5	75	90	71
CpMe$_4$R (%)	24	65	65	14	6	14
Cp (%)	54	30	29	11	3	15

Table S11 β-fragment molecular orbital analysis of Re(Cp)(CpMe$_4$R), where R = CHCH$_2$ (**4**)

β MO	HOMO-4	HOMO-3	HOMO-2	HOMO-1	HOMO	LUMO
Energy (eV)	-7.35	-6.21	-5.94	-4.91	-4.57	-2.36
Re (%)	13	5	6	74	91	71
CpMe$_4$R (%)	34	62	75	15	6	15
Cp (%)	54	32	20	11	3	14

Table S12. β-fragment molecular orbital analysis of Re(Cp)(CpMe$_4$R), where R = CHO (**5**)

β MO	HOMO-4	HOMO-3	HOMO-2	HOMO-1	HOMO	LUMO
Energy (eV)	-6.75	-6.63	-6.46	-5.28	-4.89	-2.66
Re (%)	1.51	3	5	73	89	72
CpMe$_4$R (%)	89	69	62	17	7	14
Cp (%)	9	27	33	10	4	14

Table S13. β-fragment molecular orbital analysis of Re(Cp)(CpMe$_4$R), where R = OMe (**6**)

β MO	HOMO-4	HOMO-3	HOMO-2	HOMO-1	HOMO	LUMO
Energy (eV)	-7.31	-6.16	-6.10	-4.89	-4.56	-2.29
Re (%)	5	5	5	75	91	71
CpMe$_4$R (%)	74	64	64	14	6	15
Cp (%)	21	31	31	11	3	14

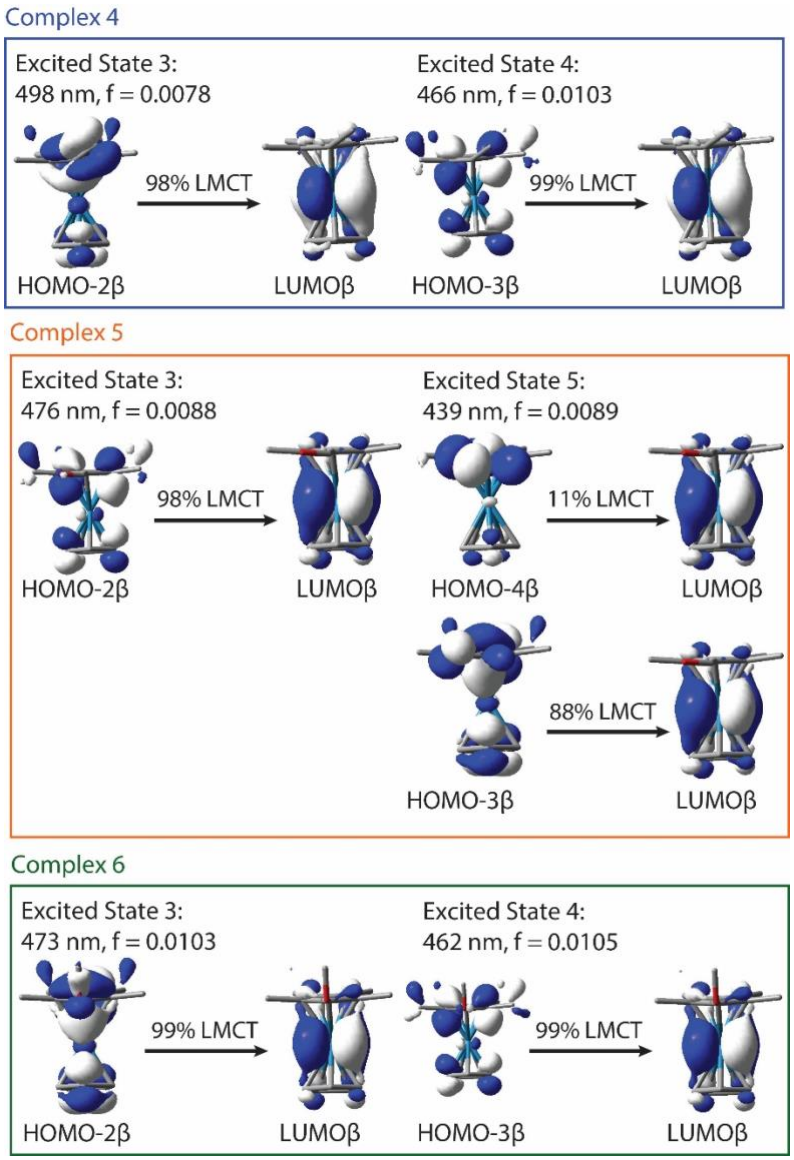

Figure S7. Donor and acceptor orbitals of the lowest energy excited states for complexes **4-6**. Calculated excitation energies (in nm) and oscillator strengths (f) for each electronic transition are provided. The percent contribution of the displayed hole-particle pair determined from the excitation coefficients obtained from the TD-DFT calculations is also provided.

Table S14. Excited states for **1**. Excited states were characterized for wavelengths > 400 nm with oscillator strength (f) ≥ 0.00

State	Hole	Particle	Coefficient (%)	Energy, nm	Energy, eV	f	Character
1	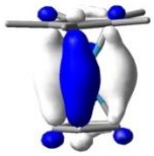	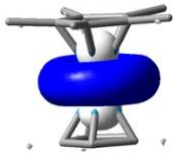	2	9834.86	0.126	0.0000	MC
		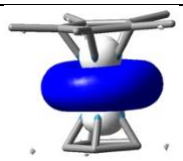	98				MC
2		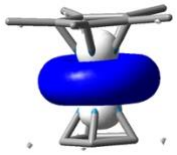	98	9672.72	0.128	0.0000	MC
		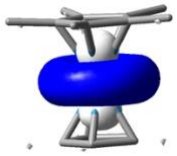	2				MC
3	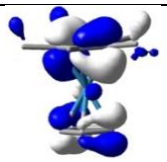	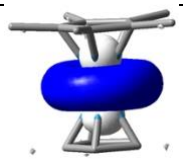	91	517.55	2.396	0.0034	LMCT
	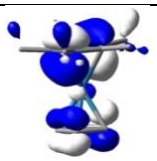	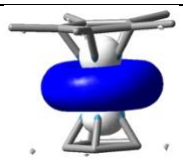	8				LMCT
4	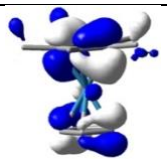	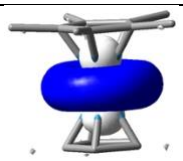	8	517.53	2.396	0.0029	LMCT
	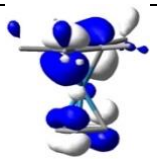	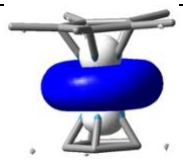	91				LMCT

Table S15. Excited states for **2**. Excited states were characterized for wavelengths > 400 nm with oscillator strength (f) ≥ 0.00

State	Hole	Particle	Coefficient (%)	Energy, nm	Energy, eV	f	Character
1		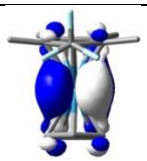	99	3044.93	0.407	0.0000	MC
2		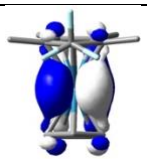	100	2127.60	0.583	0.0004	MC
3	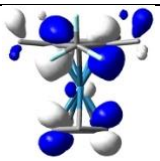	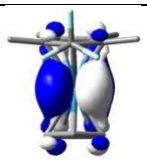	99	462.47	2.681	0.0100	LMCT
4		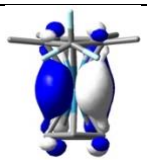	99	424.44	2.921	0.0104	LMCT

Table S16. Excited states for **3**. Excited states were characterized for wavelengths > 400 nm with oscillator strength (*f*) ≥ 0.00

State	Hole	Particle	Coefficient (%)	Energy, nm	Energy, eV	*f*	Character
1	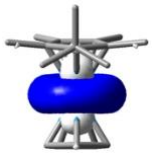		99	3109.64	0.3987	0.0000	MC
2		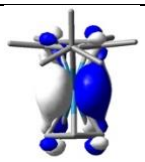	100	2378.45	0.5213	0.0002	MC
3	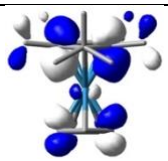	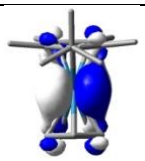	99	464.31	2.6073	0.0111	LMCT
4	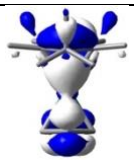	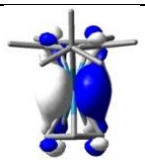	99	456.42	2.7164	0.0094	LMCT

Table S17. Excited states for **4**. Excited states were characterized for wavelengths > 400 nm with oscillator strength (*f*) ≥ 0.00

State	Hole	Particle	Coefficient (%)	Energy, nm	Energy, eV	*f*	Character
1		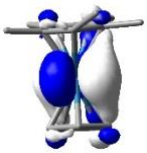	99	3431.55	0.361	0.0000	MC
2		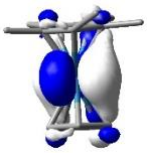	96	2746.65	0.451	0.0003	MC
3	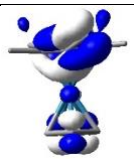	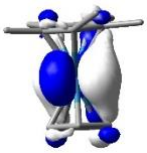	98	498.27	2.488	0.0078	LMCT
4	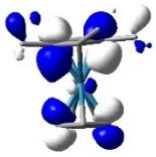	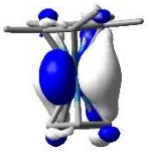	99	466.43	2.658	0.0103	LMCT

Table S18. Excited states for **5**. Excited states were characterized for wavelengths > 400 nm with oscillator strength (f) ≥ 0.00

State	Hole	Particle	Coefficient (%)	Energy, nm	Energy, eV	f	Character
1	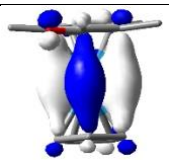		3	3396.99	0.365	0.0000	MC
	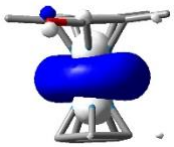		97				MC
2	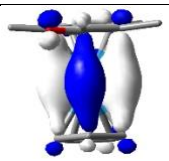		93	2286.35	0.542	0.0004	MC
	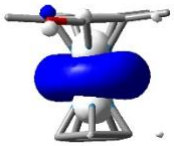		2				MC
3	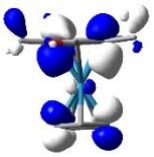		98	475.91	2.605	0.0088	LMCT
4		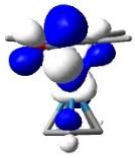	5	446.01	2.7799	0.0019	MC/MLCT
		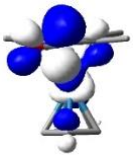	5				MC/MLCT
	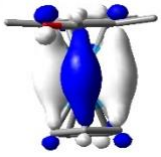	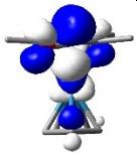	3				MC/MLCT

	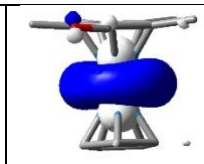	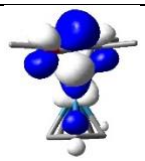	78				MC/MLCT
	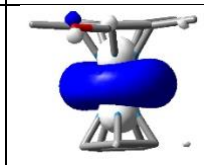	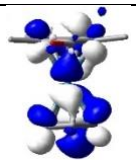	3				MC/MLCT
5	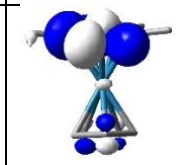	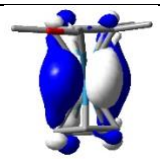	11	438.50	2.8275	0.0089	LMCT
	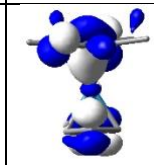	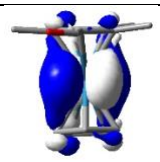	88				LMCT
6	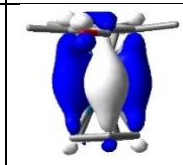	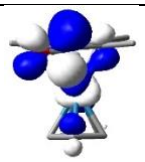	30	402.09	3.0835	0.0008	MC/MLCT
	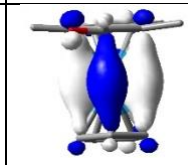	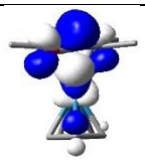	51				MC/MLCT
	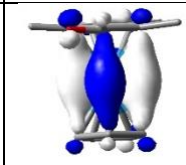	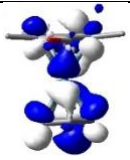	1				MC/MLCT
	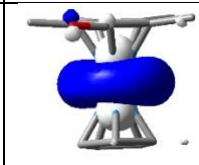	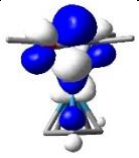	11				MC/MLCT

Table S19. Excited states for **6**. Excited states were characterized for wavelengths > 400 nm with oscillator strength (*f*) ≥ 0.00

State	Hole	Particle	Coefficient (%)	Energy, nm	Energy, eV	*f*	Character
1	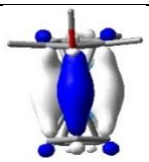	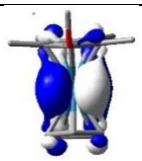	3	2904.26	0.4269	0.0000	MC
	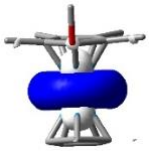		96				MC
2	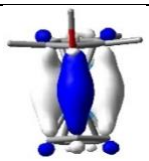	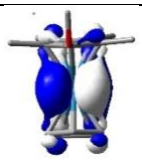	92	2520.31	0.4919	0.0002	MC
	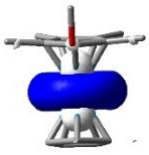	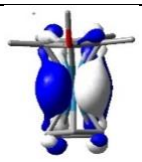	3				MC
3	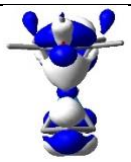	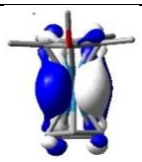	99	472.54	2.6238	0.0103	LMCT
4	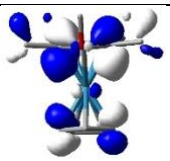	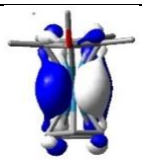	99	461.69	2.6854	0.0105	LMCT

Table S20. Table of Calculated DFT Energies

	Optimization and Frequency calculations at (U)B3LYP/6-311G*/SDD+f in benzene		Single Point Energy calculations at (U)BP86/6-311G*/SDD+f in THF
Re(Cp)($CpMe_4R$) Complexes	Electronic energies, au	Thermal Corrections to Gibbs free energies, au	Electronic energies, au
$ReCp^*_2$ (0) doublet	-858.779280998	0.385980	-858.875002617
$ReCp^*_2$ (-1) singlet	-858.851965115	0.398685	-858.980127973
1 R = Me (0) doublet	-662.122751814	0.255423	-662.231269411
1 R = Me (-1) singlet	-662.202389289	0.262090	-662.343215434
2 R = CF_3 (0) doublet	-959.953400381	0.231744	-960.063171529
2 R = CF_3 (-1) singlet	-960.039485416	0.236127	-960.183698346
3 R = ^{t}Bu (0) doublet	-780.095662017	0.341240	-780.195708162
3 R = ^{t}Bu (-1) singlet	-780.169610710	0.343473	-780.304623863
4 R = $CHCH_2$ (0) doublet	-700.219469797	0.262004	-700.323669104
4 R = $CHCH_2$ (-1) singlet	-700.299220945	0.266396	-700.439493670
5 R = CHO (0) doublet	-736.164486441	0.239257	-736.277391755
5 R = CHO (-1) singlet	-736.255829734	0.244183	-736.403125678
6 R = OMe (0) doublet	-737.350683360	0.260302	-737.459321937
6 R = OMe (-1) singlet	-737.426425326	0.264505	-737.571927169